Journal of Renewable Materials

Tech Science Press

DOI: 10.32604/jrm.2023.023721

check for updates

ARTICLE

Green Hydrothermal Synthesis and Applications of *Sorbus pohuashanensis*/*Aronia melanocarpa* Extracts Functionalized-Au/Ag/AuAg Nanoparticles

Jin Huang[1,2,#], Jixiang Sun[1,3,4,#], Kai Shao[1,3,4], Yamei Lin[1,3,4], Zhiguo Liu[1,3,4,*], Yujie Fu[1] and Liqiang Mu[2,*]

[1]College of Chemistry, Chemical Engineering and Resource Utilization, Key Laboratory of Forest Plant Ecology Ministry of Education, Northeast Forestry University, Harbin, 150040, China

[2]School of Forestry, Northeast Forestry University, Harbin, 150040, China

[3]Heilongjiang Provincial Key Laboratory of Ecological Utilization of Forestry-Based Active Substances, Harbin, 150040, China

[4]National Engineering Laboratory of Bio-Resource Eco-Utilization, Harbin, 150040, China

[*]Corresponding Authors: Zhiguo Liu. Email: zguoliu@nefu.edu.cn; Liqiang Mu. Email: mlq0417@163.com

[#]These Authors contributed equally to this work

Received: 17 June 2022 Accepted: 11 August 2022

ABSTRACT

Nanoparticles (NPs) have already been widely used in catalysis, antibacterial and coating fields. Compared with the traditional toxic and harmful reducing reagents, green synthesis of NPs by using plant extracts is not only environmental-friendly and cost-effective but also conducive to the multi-level and efficient utilization of wild plant resources. In this study, the aqueous extracts from *Sorbus pohuashanensis* (SP) and *Aronia melanocarpa* (AM) fruits were used as the reducing and protective reagents for synthesizing Au/AgNPs, with the characteristics of originality operation and high repeatability. The SP/AM fruit extracts functionalized Au/AgNPs were characterized by UV-vis spectroscopy (UV-vis), transmission electron microscopy (TEM), energy dispersive spectroscopy (EDS), scanning electron microscope (SEM), X-ray diffraction (XRD) and Fourier transform infrared spectroscopy (FTIR). UV-vis spectrums showed the NPs peaks verified by the presence between 400–550 nm; TEM and SEM demonstrated NPs displayed approximately spherical structures; EDS confirmed the existence of Au/Ag elements; XRD measurements confirmed that the obtained NPs showed highly crystalline structures; FTIR demonstrated the fruits extracts were adsorbed on the surface of NPs. Primary experiments indicated that SP/AM fruit extracts functionalized-NPs could be used as the reagents for removing the organic dyes efficiently; Zone of inhibition tests (ZOI) explained that NPs have slow-release antibacterial activity.

KEYWORDS

Green synthesis; nanoparticles; *Sorbus pohuashanensis*; *Aronia melanocarpa*; plant extracts; dye removal

Abbreviations

NPs	nanoparticles
SP	*Sorbus pohuashanensis*
AM	*Aronia melanocarpa*
AA	ascorbic acid

SP-NPs	*Sorbus pohuashanensis* functionalized nanoparticles
AM-NPs	*Aronia melanocarpa* functionalized nanoparticles
AA-NPs	ascorbic acid functionalized nanoparticles
AgNPs	silver nanoparticles
AuNPs	gold nanoparticles
AuAgNPs	gold and silver alloy nanoparticles
SP-AgNPs	*Sorbus pohuashanensis*-silver nanoparticles
AM-AgNPs	*Aronia melanocarpa*-silver nanoparticles
AA-AgNPs	ascorbic acid-silver nanoparticles
SP-AuNPs	*Sorbus pohuashanensis*-gold nanoparticles
AM-AuNPs	*Aronia melanocarpa*-gold nanoparticles
AA-AuNPs	ascorbic acid-gold nanoparticles
SP-AuAgNPs	*Sorbus pohuashanensis*-gold and silver alloy nanoparticles
AM-AuAgNPs	*Aronia melanocarpa*-gold and silver alloy nanoparticles
AA-AuAgNPs	ascorbic acid-gold and silver alloy nanoparticles
MB	Methylene blue
RhB	Rhodamine B

1 Introduction

Compared with traditional materials, nanomaterials demonstrate ideal optical, thermal, magnetic, mechanical, adsorption and catalytic properties. Besides, nanomaterials are already widely adopted in textile, coating, medical and military fields [1,2]. Traditional nanomaterials synthesis methods include physical (laser sputtering, gas evaporation, ball milling) and chemical (hydrothermal, precipitation) methods. Nanosized metal and oxides such as Au [3], Ag [4], Pt [5] and TiO_2 [6] had already been synthesized by both strategies repeatedly. Au/AgNPs also exhibit catalysis and enhanced Raman spectroscopy effect [7]. Functional NPs also exhibit physiological toxicity, while part of NPs shows better performance on antibacterial activity [8]. The chemical reduction method would utilize toxic and harmful reagents and stabilizers in most cases, which cause ecological risks and irreversible environmental damage. Intending to solve pollution, green synthesis method with energy conservation, environmental protection and low toxicity characteristics emerged under the above circumstances. In the process of synthesizing NPs, instead of toxic reducing reagents, the utilization of plant extracts or microbial metabolites could exhibit the concept of environmental protection and efficient utilization of resources [9]. Dyes are substances with bright and firm colors, which are already widely used in industry. Organic dye pollution in wastewater has recently been a severe environmental problem. Easy decomposition, instability and poor coloring ability affect the expanded exploration of natural dyes [10]. Due to the strong dyeing ability of human-made dyes, milligram levels of dyes can change water transparency and color. Among the organic dyes, methylene blue (MB) and rhodamine B (RhB) are widely used in industry and medicine. Besides, RhB showed a strong fluorescence effect [11]. Various biological, chemical and physical methods have been applied to solve the problem of water pollution caused by organic dyes. Among these different methods, functionalized nanomaterials showed rapid activity in eliminating water pollution [12–14]. Wild shrubs *Sorbus pohuashanensis* (SP) and *Aronia melanocarpa* (AM) fruits extracts contain flavonoids and polyphenols, which were used as reducing reagents and stabilizers reagents for synthesizing functionalized-NPs, to achieve the multi-level and efficient utilization value [15]. The chemically modified nanomaterials demonstrate the physical and chemical activities in the experiment. Abundant wild plants' fruit resources were not explored for metal NPs synthesis, including the *Sorbus pohuashanensis* (SP) and *Aronia melanocarpa* (AM) plants. The utilization of NPs has been

gradually developed and created, including the removal activity of toxic and harmful organic dyes from aqueous solutions [13]. Functionalized-NPs usually have a high surface area while specific organic dye removal effects [16]. However, part of the adsorbents still have troubles, such as insufficient adsorption capacity and complex synthesis processes, which is still challenging to select and synthesize the ideal reagents with simple structure and high-removal efficiency character. In this research, SP and AM fruits water extracts were used for synthesizing 6 kinds of NPs (SP-AgNPs, AM-AgNPs, SP-AuNPs, AM-AuNPs, SP-AuAgNPs, AM-AuAgNPs). Furthermore, primary research needs to characterize the properties and further application of SP/AM-NPs after the preliminary synthesis process.

2 Materials and Methods

2.1 Materials

Sorbus pohuashanensis fruits (purchased from Xunke county, Heilongjiang province, China); *Aronia melanocarpa* fruits (purchased from Dalian City, Liaoning Province, China); Milli-Q water (electrical resistivity value ≥ 18.2 MΩ·cm); silver nitrate, chloroauric acid, hydrochloric acid, sodium hydroxide, ascorbic acid (AA), sodium dodecyl benzene sulfonate, methylene blue (MB), rhodamine B (RhB), penicillin, nutritious broth and agar were purchased from Sinopharm. The *E. coli* (Gram-negative, ATCC8739), *C. albicans* (Fungi, ATCC16404) and *S. aureus* (Gram-positive, ATCC6538) used in ZOI experiments were purchased from the Institute of Applied Microbiology, Heilongjiang Academy of Agricultural Sciences, China.

2.2 Methods of NPs Synthesis

2.2.1 Preparation of SP/AM Fruits Extracts

SP and AM fruit extracts were obtained from the fresh fruits. The preparation processes included removing branches, water-cleaning, oven-drying, crushing and Milli-Q water extraction. 100 ml Milli-Q water and 1.00 g SP/AM powder were mixed smoothly in a beaker. The solid-liquid mixed mixture was boiled under stirring conditions for 30 min. The supernatant was obtained by centrifugation process and diluted to 100 ml finally. The SP and AM fruits water extracts presented yellow and purple, respectively. Meanwhile, fruit extracts were stored in the refrigerator under the condition of 2°C–8°C for further synthetic experiments.

2.2.2 Synthesis Conditions on SP/AM/AA-NPs

In SP/AM-NPs synthesis experiments, the mixture solution pH value, material ratio (v/v), heating temperature and heating time need to be optimized by UV-vis, TEM and SEM characterization results. According to previous research, setting pH values are 3, 5, 7, 10 and 11; the material ratios (v/v) are 1:5, 1:10, 1:20 and 1:30; heating temperatures are 60°C, 100°C, 140°C and 180°C; heating time is 1, 2, 3 and 4 h; for accelerating the reaction efficiency, NPs were synthesized in the ovens by hydrothermal method. The method for preparing NPs solid powder was designed based on the following procedures: centrifuging NPs colloids (10,000 r/min for 20 min), discarding the supernatant, and the remaining solids were dried at 40°C in the oven for 4–6 h. Fig. 1 shows the diagram of fruits extracts preparation and NPs synthesizing processes.

Furthermore, the common organic reducing reagent ascorbic acid (AA) was also used to synthesize NPs simultaneously. For comparison, AA-NPs were also synthesized with 1% ascorbic acid solution and metal ions solution at the same mass concentration. The specific synthesis conditions are as follows: (1) Synthesis conditions on AA-AgNPs: Mixing 20 ml AA solution (1%), 20 ml Milli-Q water, 0.5 ml sodium dodecyl benzene sulfonate (10%), 2 ml $AgNO_3$ (1%) in sequence, then adjusting solution pH to 9 by NaOH; (2) Synthesis conditions on AA-AuNPs: Mixing 20 ml AA solution (1%), 10 ml Milli-Q water and 2 ml $HAuCl_4$ (1%) in sequence; (3) Synthesis conditions on AA-AuAgNPs: Mixing 20 ml AA solution (1%), 10 ml Milli-Q water, 2 ml $HAuCl_4$ (1%) and 2 ml $AgNO_3$ (1%) in sequence. Because of

the stronger reducibility of AA than fruit extracts, to produce stable NPs, heating cannot be adjusted during the whole reaction.

Figure 1: The diagram of the preparation of fruits extracts and SP/AM-NPs synthesizing processes

2.3 Characterization of SP/AM-NPS

2.3.1 UV-vis Absorption Spectra (UV-vis)

After the synthesis process, SP/AM-NPs colloids were diluted with Milli-Q water appropriately and added to the quartz cuvette for UV-vis measurement (Persee TU-1901). UV-vis spectrophotometer recorded all datum over the range of 200–700 nm; Meanwhile, the SP and AM fruits water extracts were also measured.

2.3.2 Transmission Electron Microscopy and Energy Dispersive Spectroscopy (TEM and EDS)

The appearance of SP/AM-NPs was measured by transmission electron microscope equipped with energy dispersive spectroscopy (HITECH HT7800 and JEOL JEM-2100). 10–50 μL SP/AM-NPs colloids were dried on carbon-copper compound round grids at room temperature for TEM and EDS analysis.

2.3.3 Scanning Electron Microscope (SEM)

For observing the morphology and structure of SP/AM-NPs, SP/AM-NPs powder was measured by scanning electron microscope (JSM-7500F). The whole test prepared 10–100 mg SP/AM-NPs powder for SEM characterization. SP/AM-NPs powder was sputtered with pure platinum in the sputtering metal instrument to enhance the conductivity.

2.3.4 Fourier Transform Infrared Spectroscopy (FTIR)

300 mg dry KBr with 2–5 mg SP/AM-NPs or SP/AM fruits extracts powder was ground together for a few minutes in the agate mortar. Then 80–100 mg mixture was pressed into slices to be tested by FTIR spectrophotometer (Thermo Nicolet-IS10).

2.3.5 X-Ray Diffraction (XRD)

SP/AM-NPs colloid solid crystal structures were measured by X-ray diffraction (Shimadzu XRD-6100). SP/AM-NPs solid samples were collected on the glass for measurements. XRD tests recorded datum over the range of 4°–90°.

2.4 Organic Dyes Removal Activity

The dye removal activities of SP/AM/AA-NPs were also analyzed. Under the appropriate dilution condition, mixing 5 ml colloids, 5 ml Milli-Q water and 0.5 ml MB solution (100 mg/L)/RhB solution (100 mg/L), respectively. After abundant shaking and mixing, centrifuge 15 min (9000 r/min) to extract

all the supernatant. During the absorption research, mixing and shaking processes were kept in the dark incubation to avoid external light. To confirm the adsorption of SP/AM/AA-NPs on organic dyes, considering the concentration change of dyes after mixing with the colloids, 1–5 mg/L MB/RhB organic dye standard working curves and blank control groups were prepared. The concentration changes of MB and RhB dyes in the supernatant before and after removal were detected by UV-vis and fluorescence spectrophotometry, respectively. Meanwhile, the removal efficiencies of colloids were calculated according to the dye concentration changes. AA-NPs also performed the comparative test on the dye removal effect under the same experimental conditions.

Furthermore, the adsorption kinetic of organic dyes by SP/AM-NPs was also analyzed in the following tests. 5 mL SP/AM-NPs colloids and 0.5 ml MB (100 mg/L)/RhB (100 mg/L) dyes solution were mixed and stirred in the shaker, and setting adsorption time was 0, 20, 40, 60, 80, 100, 120, 140 and 160 min, respectively. After incubation, the solutions were centrifuged to observe the dye concentration difference during the adsorption process. MB and RhB standard curves were established from a series of the given standard solutions; MB removal rates were measured by the UV-vis spectrophotometer (Persee TU-1901, absorption λ = 665 nm); RhB removal rates were measured by a fluorescence spectrophotometer (Hitachi F-7000, excitation λ = 262 nm, emission λ = 580 nm). Organic dye removal rate (%) = $[(C_0 - C_1)/C_0] \times 100\%$ (C_0: initial dye concentration of the mixed solution, C_1: after incubation dye concentration of mixed solution).

2.5 Zone of Inhibition (ZOI)

A zone of inhibition test was applied for antibacterial activity measurement, including 14 kinds of colloids/solutions (SP/AM/AA-NPs, SP/AM fruits extracts, penicillin sodium (0.1%), $AgNO_3$(1%) and $HAuCl_4$(1%)) were studied simultaneously. Under germ-free conditions, the bacteria/fungus (10^8 CFU/ml) was inoculated onto round cell culture dishes containing solid agar. In sequence, sterile paper pieces with liquid to be tested (10 μl) onto round cell culture dishes. *E. coli* and *S. aureus* dishes were incubated at 37°C for 24 h; *C. albicans dish* were incubated at 28°C for 24 h.

3 Results and Discussions

3.1 UV-vis Absorption Spectra Characterization

UV-vis measurements (Fig. 2) show that AgNPs, AuNPs and AuAgNPs colloids had peaked at 410, 540 and 430 nm, respectively. The peak curves show that Au/AgNPs colloids had been synthesized; The absorption spectrum curves of SP-NPs and AM-NPs were similar in appearance. The absorption spectrum peaks of NPs colloids are generated by plasma resonance on the surface of NPs [17]. Heating is conducive to the reaction's rapid completion and the crystal nucleus's growth in the reaction process [18]. After repeated experiments, the proper solution pH values, heating time, reaction temperature and material ratios (v/v) were finally selected. In synthesizing NPs, pH value and heating degree were the key factors, while the material ratios did not show a noticeable effect. Appropriate pH value was the critical factor in the hydrothermal reaction: colloids would not react or produce flocculent precipitation under acidic pH conditions. However, the strong alkaline situation would lead to rapid reduction of metal ions with extensive precipitation or bad shape. High temperature or long heating time would lead NPs to excessive collision and aggregation, and the visible precipitations would separate from colloids. Furthermore, if the NPs solution precipitated after heating during the hydrothermal reaction, the reaction conditions should be readjusted. When the heating temperature was 180°C, it would lead to the carbonization of fruit extracts. The high reaction temperature and fast heating rate make NPs form large, excessive precipitations. Since $HAuCl_4$ is easier to be reduced than $AgNO_3$, the required reaction time and heating temperature must be appropriately diminished. Otherwise, AuNPs are more likely to precipitate than AgNPs. In synthesizing AuNPs, pink flocculent precipitation would be produced in the condition of strong acid (pH < 2.5); Besides, AuNPs could form more distinct shapes in the state of weak acid than in neutral and alkaline conditions.

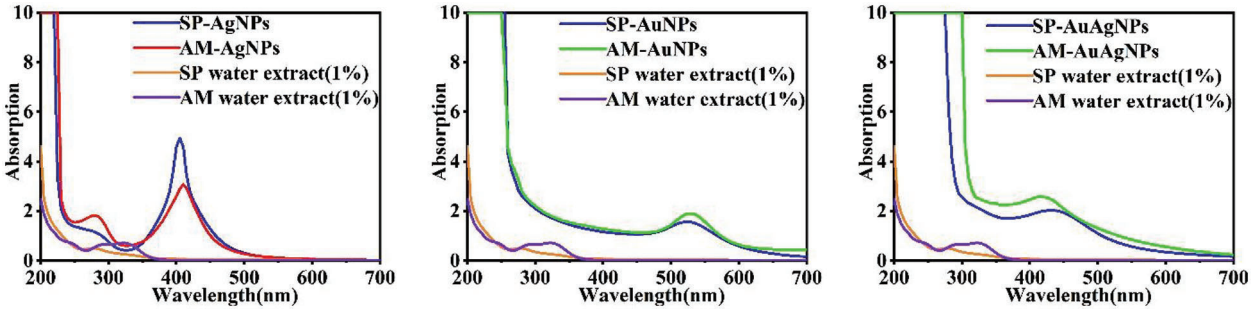

Figure 2: UV-vis characterization spectrums of SP/AM-NPs and SP/AM fruits extracts

3.2 TEM and EDS Characterization

TEM characterization pictures (Fig. 3) confirm that: the NPs shape showed an approximately spherical structure; The smaller average particle size of AuNPs and Au/AgNPs was due to shorter heating time and lower temperature of the hydrothermal reaction. Au/AgNPs pictures showed AgCl crystal emerged (triangular, square and rod-shaped). EDS characterization confirmed the existence of gold/silver elements. The carbon, silicon and other elements originated from fruit extracts. The plants' fruit extracts were used as the reducing reagents and stabilizers, which proved to be environmental-friendly, low-cost and quickly produced. Table 1 shows the average particle sizes of NPs varied from 11.45 to 36.79 nm, which belong to the nanomaterial size standard; The increase in heating time is conducive to forming crystals with larger particle sizes.

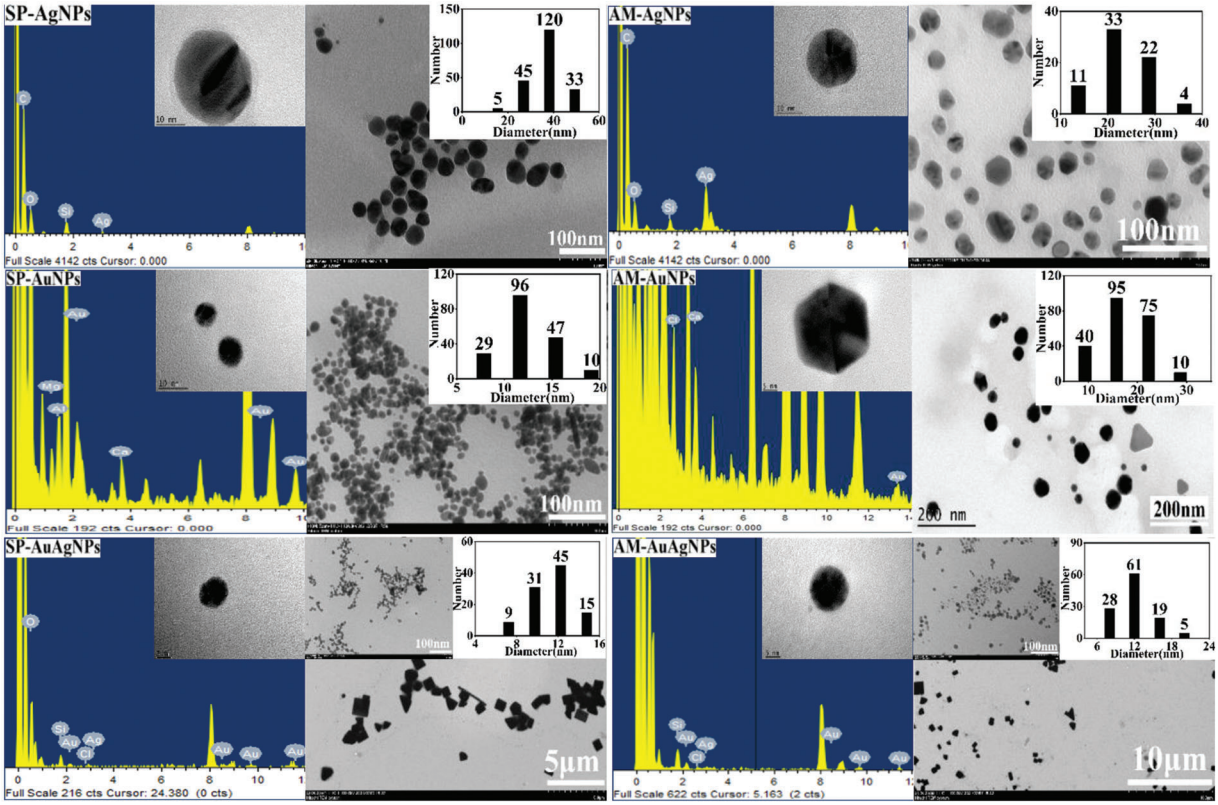

Figure 3: TEM and EDS characterization pictures of SP/AM-NPs

Table 1: Particle size statistics of spherical SP/AM-NPs (n > 100)

No.	Types of NPs	Maximum particle size (nm)	Minimum particle size (nm)	Average particle size (nm)
1	SP-AgNPs	69.08	14.35	36.79 ± 7.30
2	AM-AgNPs	38.44	13.65	23.54 ± 5.44
3	SP-AuNPs	19.93	7.08	12.45 ± 2.63
4	AM-AuNPs	44.07	6.86	17.48 ± 4.88
5	SP-AuAgNPs	15.56	6.99	11.45 ± 1.98
6	AM-AuAgNPs	20.06	6.39	12.15 ± 2.86

3.3 SEM Characterization

SEM characterization pictures (Fig. 4) indicate the microstructure of NPs was spherical, which coincided with the characterization result from TEM. Consistent with the TEM characterization results, due to the simultaneous usage of $HAuCl_4$ and $AgNO_3$, large numbers of AgCl crystals formed in the colloids. The AgCl crystals present cubic, triangle and rod-shaped. However, some spherical Au/AgNPs also emerged beside the AgCl crystal. However, the formation of AgCl crystal is not conducive to the reducing formation process of Au/AgNPs. According to the UV-vis, TEM and SEM characterization results, after sufficient optimizing trials, the proper and suitable synthesizing conditions of SP/AM-NPs were selected in Table 2. Fig. 5 demonstrates the pictures of dry fruits and powder; Part of the differences between SP and AM fruits water extracts composition would lead to the diversity of synthesizing conditions.

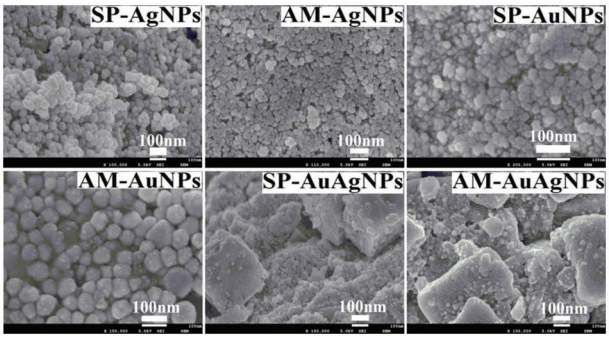

Figure 4: SEM characterization pictures of SP/AM-NPs

Table 2: The synthesis conditions on SP/AM-NPs

No.	Types of NPs	Reducing reagent solutions	Metal salt solutions	Reaction conditions
1	SP-AgNPs	SP fruits extracts (1%) 20 ml and Milli-Q water 20 ml	$AgNO_3$ (1%) 2 ml	Adjust the reaction solution pH = 7 with NaOH, stir for 30 min, and heat the reaction kettle at 140°C for 3 h
2	AM-AgNPs	AM fruits extracts (1%) 20 ml and Milli-Q water 20 ml		Adjust the reaction solution pH = 7 with NaOH, stir for 30 min, and heat the reaction kettle at 140°C for 4 h

(Continued)

Table 2 (continued)

No.	Types of NPs	Reducing reagent solutions	Metal salt solutions	Reaction conditions
3	SP-AuNPs	SP fruits extracts (1%) 20 ml and Milli-Q water 10 ml	$HAuCl_4 \cdot 4H_2O$ (1%) 2 ml	Adjust the reaction solution pH = 5 with HCl, stir for 30 min, and heat the reaction kettle at 100°C for 1 h
4	AM-AuNPs	AM fruits extracts (1%) 20 ml and Milli-Q water 10 ml		Adjust the reaction solution pH = 3 with HCl, stir for 30 min, and heat the reaction kettle at 100°C for 1 h
5	SP-AuAgNPs	SP fruits extracts (1%) 20 ml and Milli-Q water 10 ml	$HAuCl_4 \cdot 4H_2O$ (1%) 2 ml and $AgNO_3$(1%) 2 ml	Adjust the reaction solution pH = 10 with NaOH, stir for 30 min, and heat the reaction kettle at 100°C for 1 h
6	AM-AuAgNPs	AM fruits extracts (1%) 20 ml and Milli-Q water 10 ml		Adjust the reaction solution pH = 11 with NaOH, stir for 30 min, and heat the reaction kettle at 100°C for 1 h

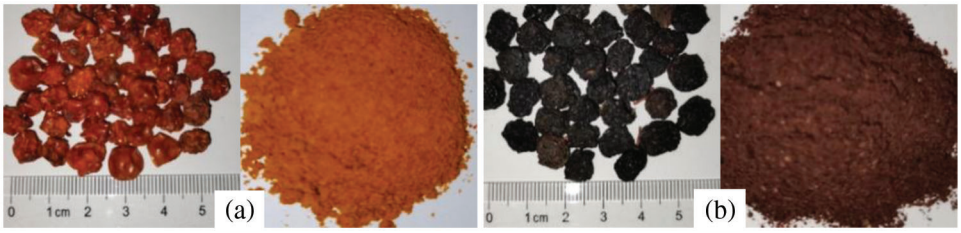

Figure 5: (a) Dry fruits and dry powder of *Sorbus pohuashanensis* (b) Dry fruits and dry powder of *Aronia melanocarpa*

3.4 FTIR Characterization

Fig. 6 demonstrates the FTIR spectrums of NPs powder; SP and AM were also measured for comparison. The FTIR results of SP-NPs and AM-NPs spectra were similar to those of the SP and AM extracts powder; the fruit extracts were attached to the crystal surface of NPs during the reaction process. Meanwhile, the NPs were chemically modified in the hydrothermal synthesis process. The broad peaks ranging from 3650 to 3000 cm^{-1} were attributed to the polyphenols hydroxyl –OH bond, which is associated with SP/AM fruits extracts [19]; 1630 cm^{-1} absorption peaks were associated with the C=C bond of benzene; 2942 and 1404 cm^{-1} absorption peaks derived from C–H bond; 1738 cm^{-1} absorption peaks were originated from C=O; The absorption peaks at 1265 cm^{-1} were bound to the O–H bond; The 1074 cm^{-1} peaks showed the stretching vibration of the C–O bond [15,20,21]; FTIR spectrums indicated that NPs surface contained SP/AM fruits extracts component preliminarily, which also indicated the specific interaction between NPs and polyphenols of fruits extracts. The fruit extracts FTIR peaks originated from the active composition (polyphenols, flavonoids and polysaccharides). Besides, the NPs powder peaks came from coating chemically active substances from fruit extracts. Hydrothermal reaction time and higher heating temperature contribute to the interaction between SP/AM fruit extracts and NPs surfaces.

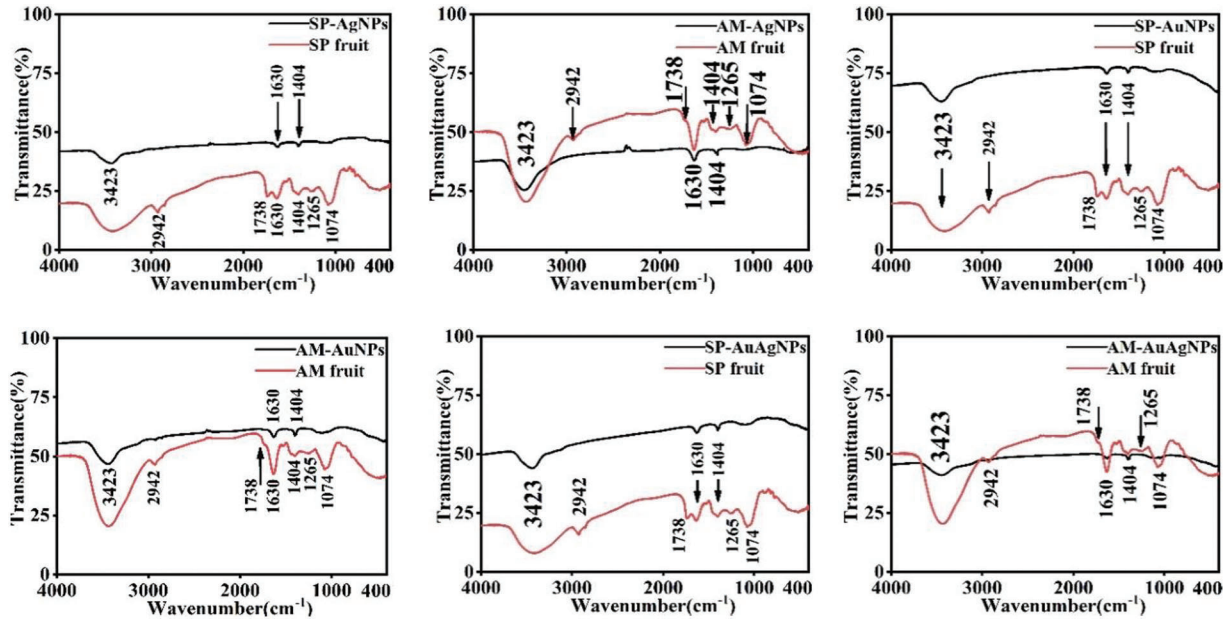

Figure 6: FTIR characterization pictures of SP/AM-NPs and SP/AM fruit extracts powder

3.5 XRD Characterization

Fig. 7 shows the AgNPs diffraction peaks at 38.1°, 44.3°, 64.4°, 77.5° and 81.5°, which respectively correspond with cubic Ag crystal structure planes of (100), (200), (220), (311) and (222) [22] (JCPDS No. 04-0783); AuNPs diffraction peaks at 38.2°, 44.4°, 64.6°, 77.5° and 81.7°, which respectively corresponding with cubic Au crystal structure planes of (100), (200), (220), (311) and (222) [23] (JCPDS No. 04-0784); AuAgNPs not only include Au/Ag peaks but also showed diffraction peaks of cubic AgCl crystal structure (JCPDS No. 31-1238). In synthesizing Au/AgNPs colloids, $HAuCl_4$ and $AgNO_3$ form part of AgCl precipitation as a by-product, showing AgCl peak type. XRD results confirmed that water-soluble metal salts $AgNO_3$ and $HAuCl_4$ could be reduced to AgNPs and AuNPs by SP and AM fruit extracts because reduced product NPs have the Au/Ag crystal structure. Furthermore, from the perspective of XRD results, there is no significant difference between SP-NPs and AM-NPs crystals.

3.6 Organic Dyes Removal Activity Results

The organic dye removal activity of SP/AM/AA-NPs colloids was tested simultaneously. Fig. 8 shows the UV-vis spectrums of MB solutions before and after interaction with NPs colloids; Fig. 9 exhibits the fluorescence spectrums of Rhodamine B (RhB) solution before and after interaction with NPs colloids. According to the removal experiments, NPs colloids showed MB/RhB removal activities. Unlike the previous research, to improve the reaction rate, removal efficiency and operation convenience, NPs colloids were mixed with the tested organic dyes directly and incubated for the predefined time for measurement. The experimental results show SP/AM/AA-NPs colloids exhibit excellent activity in efficiently removing MB and RhB organic dyes. Too long a heating time would lead to multiple intense collisions of particle size and the formation of significant particle precipitation; However, too short a heating time could result in unstable nanoparticles. Meanwhile, the two cases do not exhibit the large specific surface area of nanoparticles with the characteristic of dye removal.

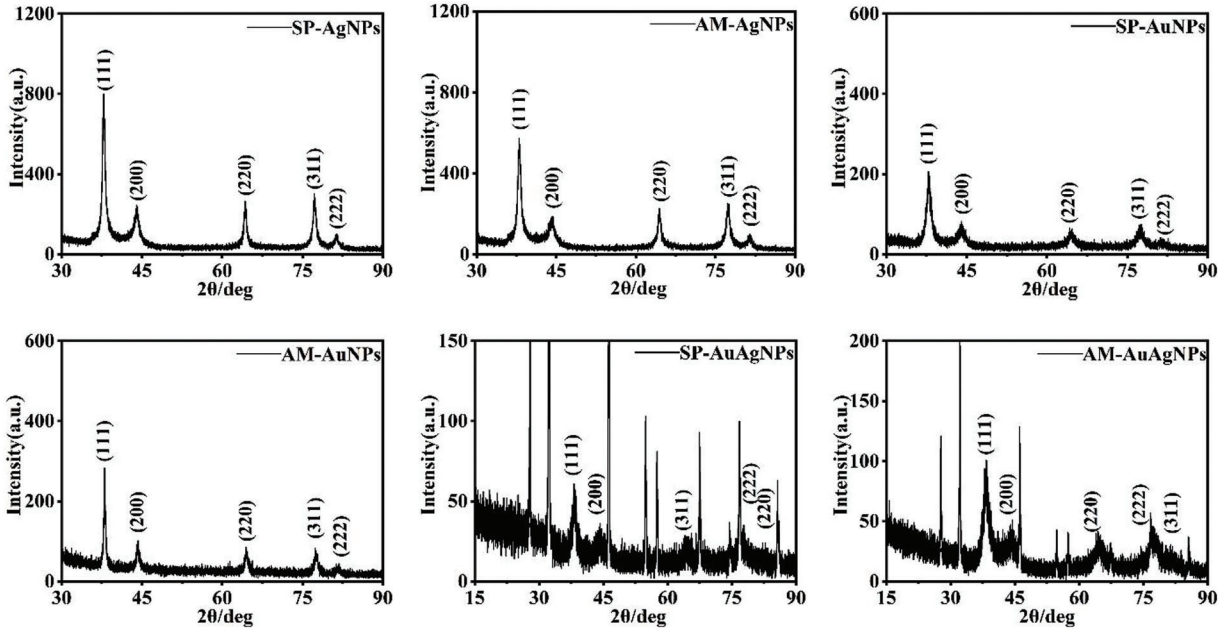

Figure 7: XRD characterization pictures of SP/AM-NPs powder

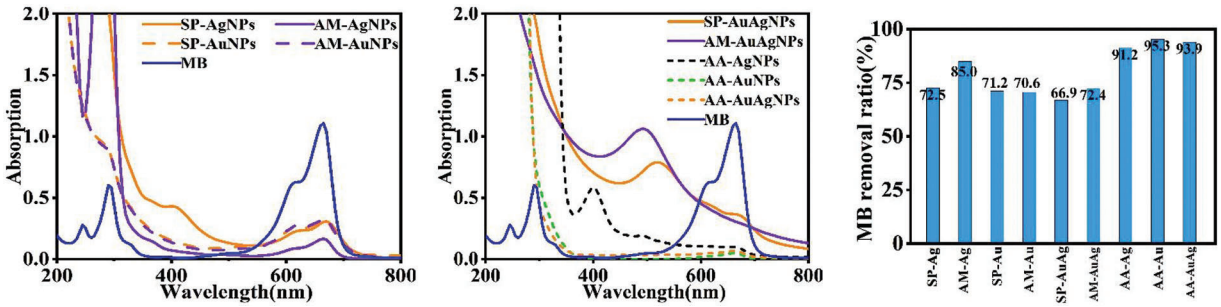

Figure 8: MB removal UV-vis spectrums and ratios by SP/AM/AA-NPs

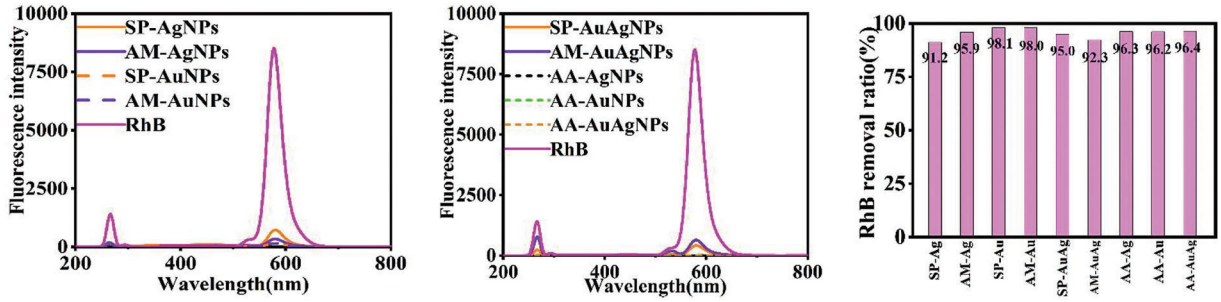

Figure 9: RhB removal fluorescence spectrums and ratios by SP/AM/AA-NPs

The adsorption kinetic on organic dyes could be researched by pseudo-first-order or pseudo-second-order models [21]. The following equations investigated the kinetic models:

The pseudo-first-order model: $\ln(q_e - q_t) - \ln q_e = -k_1 t$;

The pseudo-second-order model: $t/q_t = 1/(k^2 \cdot q_e^2) + t/q_e$.

Notes: t indicates the adsorption time; q_e indicates adsorption capacity in the equilibrium state; q_t indicates the adsorption capacity at the adsorption time; k_1 indicates the rate constant of the pseudo-first-order; k_2 indicates the rate constant of pseudo-second-order. According to the experimental results, the kinetic model of pseudo-second-order correlation coefficient (R^2) calculated showed close to 1 (Fig. 10), which demonstrated the adsorption of MB and RhB organic dyes by SP/AM-NPs all belong to the second-order kinetic (chemical adsorption process). Meanwhile, observation through the time curves, the dye adsorption process was completed instantly.

Referring to previous research results, the mechanism of SP/AM-NPs eliminating organic dye could be separated into two kinds of modes, adsorption removal and induced degradation [10,20,21]. The vast surface area of NPs could adsorb organic dyes through a hydrogen bond, van der Waals force and electrostatic interaction. The phenolic hydroxyl groups attached to the surface of NPs could also interact with dye molecules [24]; under the condition of photocatalytic oxidation, NPs colloids could induce the generation of hydroxyl radicals, which lead to the degradation of dye molecules [25]. The organic dye adsorption processes were performed in dark incubation to avoid sunlight-induced reactions. The NPs removal activities were related to the strength of the chemical bond between metal nanoparticles and fruit extracts. Fig. 11 generally describes the schematic diagram of the proposed mechanism of SP/AM-NPs eliminating organic dyes. Due to the ideal dye-eliminating activities of SP/AM-NPs, these material colloids could be developed as new reagents for dye removal tasks.

3.7 ZOI Characterization

Fig. 12 presents the zone of inhibition (ZOI) results; the antibacterial activities of the 14 samples were investigated simultaneously by the disk diffusion approach. ZOI showed that NPs have slow-release antibacterial activities. Meanwhile, the antibacterial activity of NPs was positively correlated with the number of metal ions added in the process. Penicillin held strong antibacterial activity. Meanwhile, the antibacterial effect of $HAuCl_4$ and $AgNO_3$ was slightly lower than that of penicillin, but they still exhibit strong antibacterial properties. However, SP/AM fruit extracts did not inhibit bacteria. Compared with $HAuCl_4$ and $AgNO_3$, Au/AgNPs colloids retain less biological toxicity with specific antibacterial properties; Au^{3+}/Ag^{+} cannot be used as antibacterial agents directly because of the biological toxicity of soluble metal salts ions. According to the antibacterial comparative experiment results, AA-NPs showed similar antibacterial effects to SP/AM-NPs. Besides, the antibacterial activities of metal NPs originate from the guidance of reactive oxygen species under certain conditions [26].

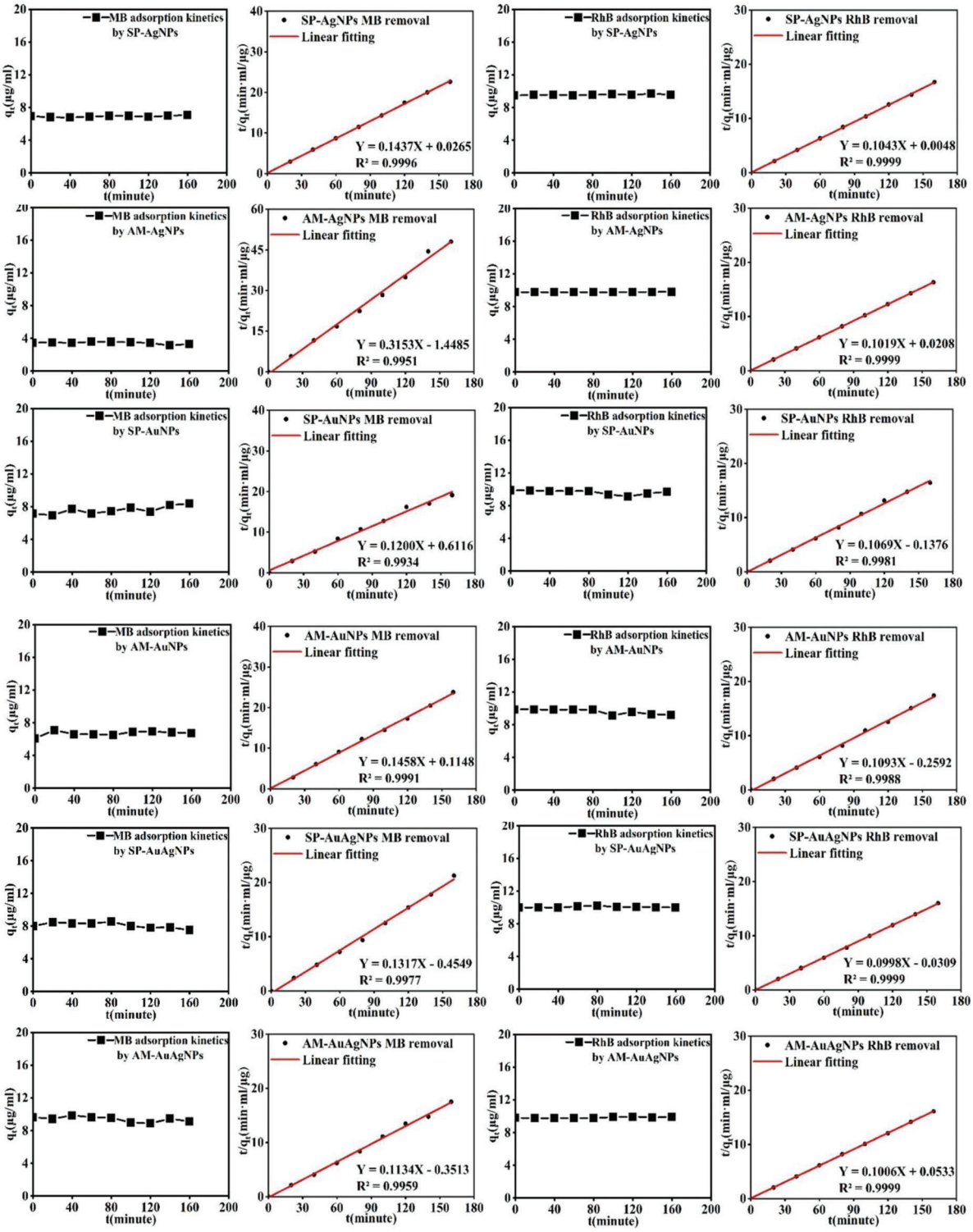

Figure 10: The pseudo-second-order kinetic models for dye adsorption by SP/AM-NPs

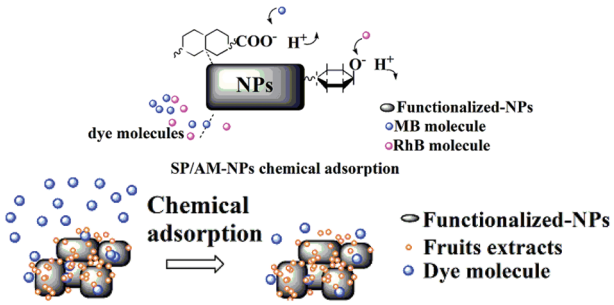

Figure 11: The schematic diagrams of the proposed mechanism for dye removal by SP/AM-NPs

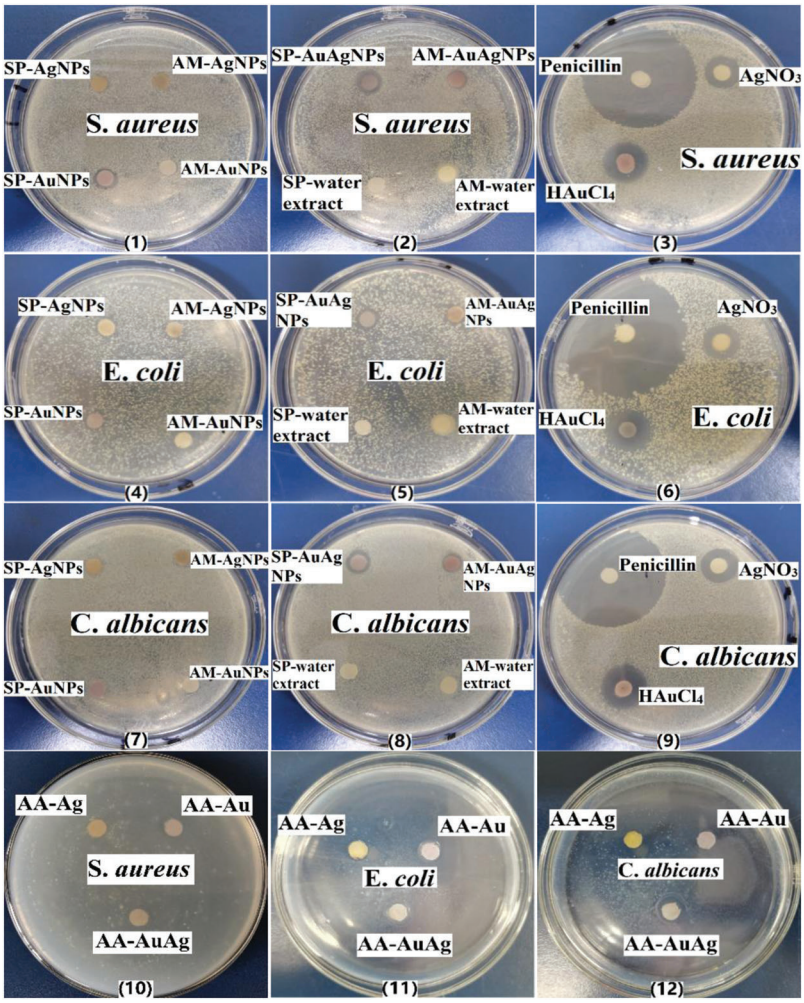

Figure 12: Zone of inhibition characterization of SP/AM/AA-NPs, SP/AM fruits extracts, penicillin (0.1%), $AgNO_3$ (1%) and $HAuCl_4$ (1%)

4 Conclusions

In this research, the green hydrothermal method synthesized the *Sorbus pohuashanensis* and *Aronia melanocarpa* extracts functionalized NPs. The green hydrothermal synthesis method proved to be safe, environmental-protection, simple processes, cost-effective and applicable, which contributes to wild plant

resources' multi-level and efficient utilization. The functionalized Au/AgNPs were synthesized by SP and AM fruits extracts and soluble metal salts with originality, stability and repeatability characteristics. Among the hydrothermal synthesis method conditions, pH value and heating degree were vital factors. Meanwhile, longer heating time would contribute to the larger crystal size of NPs. TEM and SEM results both indicated NPs showed spherical structure; EDS demonstrated the existence of gold/silver elements; FTIR indicated NPs contain SP/AM fruits extracts component; XRD results confirmed that the NPs solid powder showed Au/Ag crystal structures; Functionalized-NPs colloids demonstrate activities on organic dyes removal, and MB/RhB organic dyes adsorption by SP/AM-NPs could be all considered as the second-order kinetic (chemical adsorption process). ZOI confirmed that NPs have moderate and slow-release antibacterial activities. The experiments demonstrated no significant differences between SP-NPs and AM-NPs in appearance, dye removal and antibacterial activities. By contrast, AA-NPs showed similar activities to SP/AM-NPs on dye removal and antibacterial tests. The SP/AM fruits extracts functionalized Au/AgNPs exhibit industrial development potential; Furthermore, the usage of plants' fruit in synthesizing nanomaterial showed conducive to the efficient utilization of wild plant resources.

Data Availability Statement: All datum that supported the findings of this research were included in the article.

Funding Statement: The authors gratefully acknowledge the financial support from the Fundamental Research Funds for the Central Universities (2572020DR07), Natural Science Fund of Heilongjiang Province (LH2019B001), the 111 Project (B20088), Heilongjiang Touyan Innovation Team Program (Tree Genetics and Breeding Innovation Team).

Conflicts of Interest: The authors declare that they have no conflicts of interest to report regarding the present study.

References

1. Polshettiwar, V., Varma, R. S. (2010). Green chemistry by nano-catalysis. *Green Chemistry, 12(5),* 743–754. DOI 10.1039/b921171c.
2. Mehdinia, A., Aziz-Zanjani, M. O. (2013). Recent advances in nanomaterials utilized in fiber coatings for solid-phase microextraction. *Trac-Trends in Analytical Chemistry, 42,* 205–215. DOI 10.1016/j.trac.2012.09.013.
3. Farooqi, Z. H., Khan, S. R., Begum, R., Ijaz, A. (2016). Review on synthesis, properties, characterization, and applications of responsive microgels fabricated with gold nanostructures. *Reviews in Chemical Engineering, 32(1),* 49–69. DOI 10.1515/revce-2015-0033.
4. Bertrand, C., Zalouk-Vergnoux, A., Giamberini, L., Poirier, L., Devin, S. et al. (2016). The influence of salinity on the fate and behavior of silver standardized nanomaterial and toxicity effects in the estuarine bivalve scrobicularia plana. *Environmental Toxicology and Chemistry, 35(10),* 2550–2561. DOI 10.1002/etc.3428.
5. Wang, J. J., Kattel, S., Wang, Z. Y., Chen, J. G. G., Liu, C. J. (2018). L-phenylalanine templated platinum catalyst with enhanced performance for oxygen reduction reaction. *ACS Applied Materials & Interfaces, 10(25),* 21321–21327. DOI 10.1021/acsami.8b04578.
6. Zhu, S. L., Xie, G. Q., Yang, X. J., Cui, Z. D. (2013). A thick hierarchical rutile TiO_2 nanomaterial with multilayered structure. *Materials Research Bulletin, 48(5),* 1961–1966. DOI 10.1016/j.materresbull.2013.01.049.
7. Zheng, Z. X., Shan, G. Y., Li, J. H., Chen, Y. W., Liu, Y. C. (2014). Au/Ag nanoalloy shells as near-infrared SERS nanoprobe for the detection of protein. *Materials Research Express, 1(4),* 045408. DOI 10.1088/2053-1591/1/4/045408.
8. Liu, J., Zhao, Z. W., Feng, H., Cui, F. Y. (2012). One-pot synthesis of Ag-Fe_3O_4 nanocomposites in the absence of additional reductant and its potent antibacterial properties. *Journal of Materials Chemistry, 22(28),* 13891–13894. DOI 10.1039/c2jm31831h.
9. Shanker, U., Jassal, V., Rani, M., Kaith, B. S. (2016). Towards green synthesis of nanoparticles: From bio-assisted sources to benign solvents. A review. *International Journal of Environmental Analytical Chemistry, 96(9),* 801–835.

10. Sarkar, S., Ponce, N. T., Banerjee, A., Bandopadhyay, R., Rajendran, S. et al. (2020). Green polymeric nanomaterials for the photocatalytic degradation of dyes: A review. *Environmental Chemistry Letters, 18(5),* 1569–1580. DOI 10.1007/s10311-020-01021-w.
11. Sharma, P., Kaur, H., Sharma, M., Sahore, V. (2011). A review on applicability of naturally available adsorbents for the removal of hazardous dyes from aqueous waste. *Environmental Monitoring and Assessment, 183(1–4),* 151–195. DOI 10.1007/s10661-011-1914-0.
12. Dalvan, R., Kianpourb, E., Tahzibi, H., Azizian, S. (2020). MgO nano-sheets for adsorption of anionic dyes from aqueous solution: Equilibrium and kinetics studies. *Surfaces and Interfaces, 21,* 100722. DOI 10.1016/j.surfin.2020.100722.
13. Alayli, A., Nadaroglu, H., Turgut, E. (2021). Nanobiocatalyst beds with fenton process for removal of methylene blue. *Applied Water Science, 11(2),* 32. DOI 10.1007/s13201-021-01367-8.
14. Wang, H. H., Zhou, P. J., Guo, R., Wang, Y. F., Zhan, H. J. et al. (2018). Synthesis of rectorite/Fe_3O_4/ZnO composites and their application for the removal of methylene blue dye. *Catalysts, 8(3),* 107. DOI 10.3390/catal8030107.
15. Gralec, M., Wawer, I., Zawada, K. (2019). *Aronia melanocarpa* berries: Phenolics composition and antioxidant properties changes during fruit development and ripening. *Emirates Journal of Food and Agriculture, 31(3),* 214–221.
16. Cheon, J. Y., Kim, S. J., Park, W. H. (2019). Facile interpretation of catalytic reaction between organic dye pollutants and silver nanoparticles with different shapes. *Journal of Nanomaterials, 2019,* 3257892. DOI 10.1155/2019/3257892.
17. Liu, Z. G., Xing, Z. M., Zu, Y. G., Tan, S. N., Zhao, L. et al. (2012). Synthesis and characterization of L-histidine capped silver nanoparticles. *Materials Science & Engineering: C, 32(4),* 811–816. DOI 10.1016/j.msec.2012.01.031.
18. Schutz, M. B., Xiao, L. S., Lehnen, T., Fischer, T., Mathur, S. (2018). Microwave-assisted synthesis of nanocrystalline binary and ternary metal oxides. *International Materials Reviews, 63(6),* 341–374. DOI 10.1080/09506608.2017.1402158.
19. Ku, C. S., Mun, S. P. (2007). Characterization of proanthocyanidin in hot water extract isolated from pinus radiata bark. *Wood Science and Technology, 41(3),* 235–247. DOI 10.1007/s00226-006-0103-8.
20. Das, C., Singh, S., Bhakta, S., Mishra, P., Biswas, G. (2022). Bio-modified magnetic nanoparticles with terminalia arjuna bark extract for the removal of methylene blue and lead (II) from simulated wastewater. *Chemosphere, 291(2),* 132673. DOI 10.1016/j.chemosphere.2021.132673.
21. Das, C., Sen, S., Singh, T., Ghosh, T., Paul, S. S. et al. (2020). Green synthesis, characterization and application of natural product coated magnetite nanoparticles for wastewater treatment. *Nanomaterials, 10(8),* 1615. DOI 10.3390/nano10081615.
22. Deng, Z. W., Chen, M., Wu, L. M. (2007). Novel method to fabricate SiO_2/Ag composite spheres and their catalytic, surface-enhanced Raman scattering properties. *Journal of Physical Chemistry C, 111(31),* 11692–11698. DOI 10.1021/jp073632h.
23. Shan, G. Y., Zhong, M. Y., Wang, S., Li, Y. J., Liu, Y. C. (2008). The synthesis and optical properties of the heterostructured ZnO/Au nanocomposites. *Journal of Colloid and Interface Science, 326(2),* 392–395. DOI 10.1016/j.jcis.2008.06.027.
24. Shaikh, W. A., Ul Islam, R., Chakraborty, S. (2021). Stable silver nanoparticle doped mesoporous biochar-based nanocomposite for efficient removal of toxic dyes. *Journal of Environmental Chemical Engineering, 9(1),* 104982. DOI 10.1016/j.jece.2020.104982.
25. Azeem, M. A. N., Hassaballa, S., Ahmed, O. M., Elsayed, K. N. M., Shaban, M. (2021). Photocatalytic activity of revolutionary galaxaura elongata, turbinaria ornata, and enteromorpha flexuosa's bio-capped silver nanoparticles for industrial wastewater treatment. *Nanomaterials, 11(12),* 3241. DOI 10.3390/nano11123241.
26. Wang, S. S., Wang, Y. Y., Peng, Y., Yang, X. M. (2019). Exploring the antibacteria performance of multicolor Ag, Au, and Cu nanoclusters. *ACS Applied Materials & Interfaces, 11(8),* 8461–8469. DOI 10.1021/acsami.8b22143.